Human Activity Classification Based on Cognitive Doppler Radar to Optimize Carrier Frequency and Sampling Rate Using Reinforcement Learning

Amin Hong, *Student Member, IEEE*, Young-Hoon Chun, *Member, IEEE*, Sangyeol Oh, and Youngwook Kim, *Senior Member, IEEE*

***Abstract*—We investigate the feasibility of using cognitive radar to increase the accuracy of human activity classification based on micro-Doppler signatures. Micro-Doppler signatures in spectrogram are influenced by various radar parameters, including carrier frequency and sampling rate. In addition, each human body motions have different speeds, which affects the quality of spectrogram. As the quality of spectrogram is the function of radar parameters as well as human motion, there exist certain radar parameters for each activity to capture the micro-Doppler signature with quality, which will ultimately enhance the classification accuracy. This article proposes to use the concept of cognitive radar that changes radar parameters depending on human motion to increase the classification accuracy when deep convolutional neural networks (DCNNs) are employed. Based on the quality of spectrogram measured, we update radar parameters of carrier frequency and sampling rate using reinforcement learning (RL) to maximize classification performance. The term image quality is defined based on the folding rate and definition rate of spectrogram. *Q*-learning was employed to adaptively change the radar parameters given the quality of spectrogram. It is verified against seven human motions that the micro-Doppler classification accuracy can be improved by the operation of cognitive radar.**

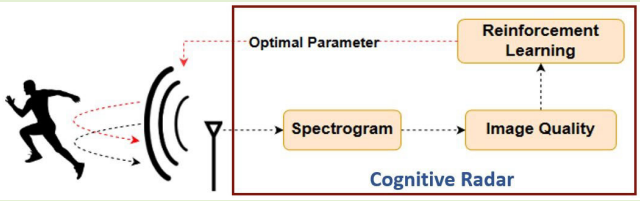

***Index Terms*—Cognitive radar, deep convolutional neural network (DCNN), human activity classification, micro-Doppler signatures, *Q*-learning, reinforcement learning (RL).**

I. Introduction

THE surge of interests in personal security and surveillance has made radar field expansion into human individual motion analysis. Detecting and classifying human individual motions through radar is highly recommended in defense, surveillance, and health care industry owing to its through-wall capability [1]. In general, human motion has been analyzed in the spectrogram, which is a joint time–frequency domain. The joint time–frequency domain that captures both temporal and frequency characteristics of the motion provides a representation of time-varying Doppler signal. Through spectrogram image, we can identify important features, such as temporal variations, frequency peaks, and energy distribution. When applied to human motion analysis, the spectrogram can provide valuable insights into the temporal dynamics and frequency characteristics of the movement.

Several classification techniques for human micro-Doppler signatures have been suggested. As micro-Doppler signatures reflect the movement of various body parts, properties, such as Doppler bandwidth, energy distribution of echoes within the envelope, and time period, can be used as features for the classification of target type and activity [2], [3]. The empirical mode decomposition (EMD) was used to extract features in [4]. EMD decomposed a Doppler signal into several components that contained a single oscillatory mode and calculated the energy of each component. Through feature vectors generated by EMD were able to classify using machine learning [4].

When it comes to image classification, deep learning has become an emerging method in a decade, and radar spectrogram classification has been no exception. The use of deep learning is a mainstream of target classification research. Popular deep learning models for radar micro-Doppler

Manuscript received 31 October 2023; revised 13 November 2023; accepted 13 November 2023. Date of publication 5 December 2023; date of current version 12 January 2024. This work was supported in part by LIG-Nex1 Company; and in part by the National Research Foundation (NRF), Republic of Korea, under Grant BK21 FOUR. The associate editor coordinating the review of this article and approving it for publication was Prof. Yuedong Xie. *(Corresponding author: Youngwook Kim.)*

Amin Hong and Youngwook Kim are with the Department of Electronic Engineering, Sogang University, Seoul 04107, South Korea (e-mail: youngkim@sogang.ac.kr).

Young-Hoon Chun and Sangyeol Oh are with LIG-Nex1, Yongin 13488, South Korea (e-mail: younghoon@ieee.org; snagyeol.oh@lignex1.com).

Digital Object Identifier 10.1109/JSEN.2023.3333407

1558-1748 © 2023 IEEE. Personal use is permitted, but republication/redistribution requires IEEE permission.
See https://www.ieee.org/publications/rights/index.html for more information.

Authorized licensed use limited to: Carnegie Mellon University Libraries. Downloaded on November 14,2025 at 13:28:53 UTC from IEEE Xplore. Restrictions apply.

classification are deep convolutional neural networks (DCNNs) [5], recurrent neural networks (RNNs) [6], and generative adversarial networks (GANs) [7]. These models are designed to learn hierarchical representations of data using multiple layers with nonlinear transformation. The hyperparameters of model architecture, such as number of layers and number of neurons per layer, and learning parameters, such as learning rate and number of epochs, impact image classification accuracy.

Not only hyperparameters of neural networks but the quality of spectrogram highly affects the classification accuracy. The quality of spectrogram is a function of radar operating parameters, such as carrier frequency, bandwidth, sampling rate, and so on. The low carrier frequency makes Doppler frequency small, while the high carrier frequency produces high Doppler frequency, which can cause aliasing. On the other hand, low sampling rate cannot capture fast-varying signatures of human motions and possibly causes aliasing. High sampling rate requires a large memory and increase computational complexity, so excessive sampling rate is not desirable. Therefore, proper radar parameters should be determined to obtain high spectrogram quality with practical feasibility, which will result in high classification accuracy. More importantly, the quality of spectrogram image is also affected by target characteristics, particularly the motion speed. Human motion classification through radar should expect various kinds of human activities. As every single human motion has different speeds of motion, there should be desirable radar parameters that result in high quality of spectrogram. It should be noted that the carrier frequency, sampling rate, and motion speed are not independent but correlated to the spectrogram quality. This fact leads that the use of fixed carrier frequency and sampling rate is not ideal. They need to be adaptively updated whenever human motion changes. To modify its radar parameter while classifying human motions, an intelligent system is required.

In this article, we propose a concept of cognitive radar to maximize the performance of DCNN that classifies human motion based on micro-Doppler signatures. While traditional radar systems typically operate with fixed radar parameters, such as frequency and bandwidth, cognitive radar is an intelligent system that changes its radar parameters depending on environment using prior knowledge gained by previous observations and databases [8], [9]. Because cognitive radar is a closed-loop system, it can iteratively optimize their resources to maximize the objective function. In general, the environment has been referred to as spectral characteristics [10]. For example, cognitive fully adaptive radar (CoFAR) was designed to adapt to complex operating environments, which incorporates multi-input multi-output waveform diversity to improve channel estimation and reduces the sample support problem that arises in nonstationary clutter cancellation application [11].

When we expand the view of environment as target characteristics like human activities, there is a possibility of applying the cognitive radar system to Doppler radar for human motion classification. To the best of our knowledge, the cognitive radar has not been applied to human micro-Doppler classification yet. First, we investigate the impact of carrier frequency and sampling rate on the classification performance using DCNN, i.e., Alexnet. This study confirms that there exists a certain range of carrier frequency and sampling rate to result in high classification accuracy. This is because there is relationship between the spectrogram quality and radar parameters. Then, we introduce the reinforcement learning (RL) to realize the cognitive radar that determines the radar parameters to enhance the classification accuracy depending on the spectrogram quality that is a function of human motion. RL is one of good approaches to implement cognitive radar because it can sequentially determine parameters based on operating environments to maximize a goal [12], [13], [14]. In RL, the agent observes the current state of the environment. According to the current state, the agent selects the action to maximize a cumulative reward. RL is effectively used in sequential optimal decision-making problems like computer games, so it would be desirable to apply RL for the implementation of the cognitive radar. In this study, we use Q-learning to update radar operation parameters depending on spectrogram quality that is a function of radar parameters as well as human motion. After training, we demonstrate that the concept of cognitive radar improves the accuracy of spectrogram classification through updating radar parameters.

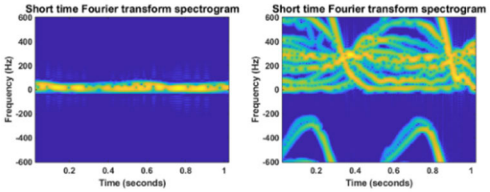

(a) (b)

Fig. 1. (a) Walk motion spectrogram $f_C = 1.5$ GHz and $f_S = 1200$ Hz. (b) Walk motion spectrogram $f_C = 30$ GHz and $f_S = 1200$ Hz.

II. Radar Parameters and Spectrogram Characteristics

When micro-Doppler signatures of human motion are captured in the spectrogram, the quality of micro-Doppler signatures depends on radar parameters, such as carrier frequency (f_C) and sampling rate (f_S) as well as the kind of human motion. Carrier frequency affects the maximum Doppler frequency (f_D) from (1), which in turn expands the spectrogram vertically

$$f_D = \frac{f_C}{c} \cdot \left(\overrightarrow{T_X} - \overrightarrow{R_X}\right) \cdot \overrightarrow{v} \tag{1}$$

where v is the velocity of a target, T_x is signal transmitted by the radar toward the target, and R_x is signal reflected back from the target. Small f_C makes the signature concentrated in low bandwidth, which will make the human motion difficult to be identified as seen in Fig. 1(a). On the other hand, very high f_C can make the signature folding due to aliasing, as seen in Fig. 1(b), which possibly negatively affect the classification performance. Therefore, a proper f_C is necessary to make the micro-Doppler signature captured with fine resolution.

In addition, according to the Nyquist sampling theorem, f_S determines the maximum human motion velocity that

Authorized licensed use limited to: Carnegie Mellon University Libraries. Downloaded on November 14,2025 at 13:28:53 UTC from IEEE Xplore. Restrictions apply.

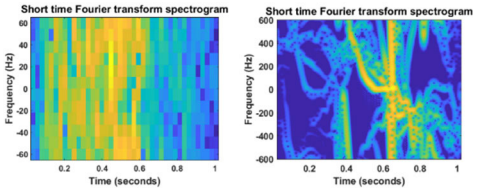

(a) (b)

Fig. 2. (a) Run motion spectrogram when $f_C = 15$ GHz and $f_S = 200$ Hz. (b) Run motion spectrogram when $f_C = 15$ GHz and $f_S = 1200$ Hz.

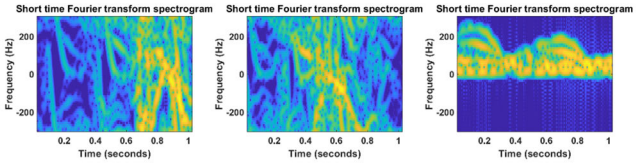

(a) (b) (c)

Fig. 3. Three human motions spectrogram when $f_C = 10$ GHz and $f_S = 600$ Hz. (a) Run. (b) Run with box. (c) Walk.

avoids the aliasing in spectrogram when fc is fixed. The aliasing makes the human motion hard to be classified. More importantly, the time resolution is determined by f_S. To represent the fast-varying human motions, fine time resolution is required. As seen in the spectrograms in Fig. 2, different time resolution shows different qualities of spectrogram for running motion. A low f_S in Fig. 2(a) cannot capture detailed Doppler variation with time, leading to blur or low-definition spectrogram. Furthermore, aliasing is observed with the low f_S. Therefore, a high f_S is desirable in general.

When it comes to classifying various human motions, the use of a fixed f_C and f_S is nonideal. As an example, three human motion spectrograms are shown in Fig. 3. From the figure, we observe that the used f_C and f_S are proper for walking motion as it shows micro-Doppler signature. However, Fig. 3(a) and (b) shows that the spectrogram of running motion is blurry and complicated because running motion is a kind of fast-moving activity that requires high f_S to capture time-varying signatures as well as to avoid aliasing.

From Figs. 1–3, it is concluded that higher f_S as well as fc will be preferable as long as aliasing does not occur. However, it requires high-specification hardware, such as high-frequency RF transceiver, high-speed analog to digital converter (ADC), large memory, and high-computational computing power, which are unnecessarily costly. In other words, finding the moderate f_S and f_C that maintain high classification accuracy will be most desirable.

III. Classification Accuracy With Radar Parameters

In this study, we focus on two radar parameters of f_S and f_C to be adaptively updated depending on human motions to enhance classification accuracy. First, in order to investigate the relationship between classification accuracy and radar parameters of f_C and f_S, we used Alexnet to estimate the classification accuracy by changing those parameters. For this test, we produce spectrogram using measured motion capture model from Carnegie Mellon University (CMU) Graphics Lab. The CMU Graphics Lab Motion Capture Database contains

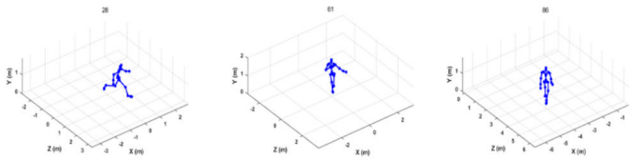

(a) (b) (c)

Fig. 4. Animated human motion. (a) Run. (b) Skipping. (c) Walk.

data measured using optical motion capture technology, where reflective markers are placed on an actor's body to track their movements. The database provides a wide range of motion sequences, such as human interaction, locomotion, and interacting with environments. Among them, we have used seven human motions (running, running with box, run to crouch, crouch to run, skipping, walking, and walk to hop to walk). Fig. 4 shows the examples of animated human motion.

To simulate the spectrogram from the motion capture database, we modeled parts of the human body, such as the torso, lower arms, lower legs, and feet with ellipsoids to generate distinct micro-Doppler signals in the resulting spectrograms. We then calculate the reflected wave from each part based on radar cross section (RCS), radar aspect angle, and the reflectivity of body. Assuming no interactions between different parts of the human body and a monostatic radar configuration, the scattered field from the human is generated by the complex sum of the RCS values of all body parts. By calculating and summing the Doppler signal from each body part, the total received wave from all body parts was constructed by superposition. The Doppler spectrogram is generated by applying the short-time Fourier transform (STFT) to the time-domain radar returns, which are obtained by measuring the reflected signals from the human target [15], [16].

Seven human motion spectrograms are simulated, where radar is placed collinearly with the motion movement. For every motion, time duration is set to 1 s. By placing the CW radar randomly in the motion movement direction, 50 spectrograms are simulated for each motion, a total of 350 spectrograms for given f_S and f_C. We simulate spectrograms by setting f_C from 312.5 MHz to 80 GHz and f_S from 10 to 2560 Hz in a logscale.

We have calculated the average classification accuracy depending on radar parameters. For a simple classification, we have used transfer learning using Alexnet [17]. The ratio between train data and validation data is 0.76:0.24. With spectrograms with different radar parameters, we have calculated the average classification accuracy. The results are shown in Fig. 5. A curve fitting tool is used in order to predict the accuracy for the rest of in-between radar parameters. The figure indicates that classification performance is a function of f_C and fs. Higher f_C tends to increase the classification performance to a certain limit. After the limit, the accuracy decreases due to aliasing. Lower f_C tends to decrease the classification because it produces unclear Doppler signatures. As far as f_S is concerned, higher f_S tends to increase the classification performance. The figure implies that

Authorized licensed use limited to: Carnegie Mellon University Libraries. Downloaded on November 14,2025 at 13:28:53 UTC from IEEE Xplore. Restrictions apply.

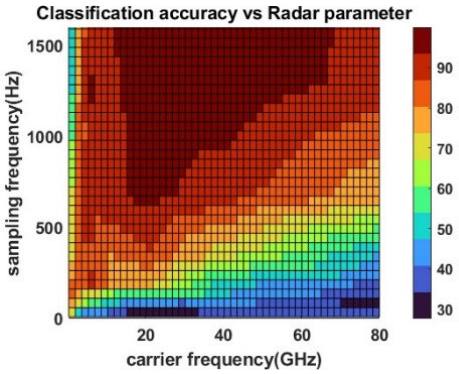

Fig. 5. Classification accuracy depending on radar parameters.

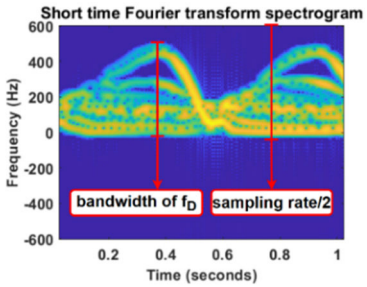

Fig. 6. Calculating folding rate.

there are ranges of f_C and f_S that maximize the classification performance. Therefore, it is reasonable to use specific radar parameters in order to achieve high classification accuracy. It should be noted that the figures are average accuracy for seven motions, while there exists specific ranges of preferable carrier frequency and sampling rate for each motion.

IV. Radar Parameters and Spectrogram Quality

To update the radar parameters to increase DCNN performance, spectrogram quality needs to be defined. The spectrogram quality will be used as an indicator that is highly correlated with classification accuracy. In this study, we define spectrogram quality by quantizing the degree of folding and the degree of definition. In order to define the degree of folding, we detect the Doppler bandwidth of f_D. When the bandwidth of f_D exceeds the half of the sampling rate, a folding occurred. We define folding rate as the ratio between the bandwidth of f_D over the half of the sampling rate as shown in the following equation. The folding rate is depicted in Fig. 6

$$\text{Folding rate} = \frac{2 \cdot f_D}{\text{Sampling rate}} \times 100. \tag{2}$$

When folding does not occur, the folding rate is lower than 100. On the other hand, when folding occurs, the bandwidth of f_D will exceed the half of the sampling rate and the folding rate exceeds 100. The maximum folding rate is when overall bandwidth of f_D is identical to sampling rate, which is set to be 200. This is because the overall bandwidth of f_D cannot exceed sampling rate although f_D will linearly increase as f_C increases.

After defining the folding rate for every human motion, we define the degree of definition of spectrogram. If the definition rate is high, image has a clear signature with resolution. Despite the fact that the definition rate can be influenced by both the sampling rate and the velocity of the specific motion, our observations revealed a strong correlation between the definition rate and the sampling rate of f_S. Therefore, we define the definition rate to be synonymous with the sampling rate as follows because the definition of spectrogram improves with the sampling rate:

$$\text{Definition rate} = \text{Sampling rate}. \tag{3}$$

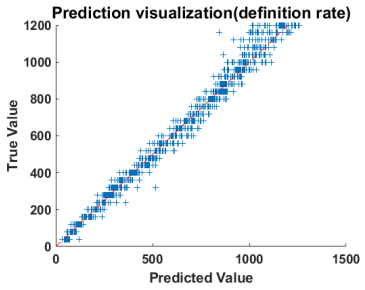

Fig. 7. Prediction performance of definition rate.

To estimate the definition rate for every human motion, we used DCNN regression model. We set f_C as 20 GHz and f_S from 120 to 1200 Hz in linear scale. For each human motion, 500 spectrograms are simulated with different sampling rates. Therefore, 3500 spectrograms are generated. In the DCNN regression model, we set input size [656 875 3] and the ratio between train data and validation data as 0.75:0.25. The model batch size is 32 and max epoch is 50. The training data consist of spectrogram and its corresponding definition rate. After DCNN training, we compared the true definition rate value and the predicted definition rate value, which is shown in Fig. 7. The RMSE of this model is 42.294.

In order to analyze the correlation between the true definition rate and the predicted definition rate, we employed Pearson correlation coefficient. This coefficient measures the strength and direction of the linear relationship between two variables, with a range from -1 to 1. A value of 1 indicates a perfect positive linear relationship. With a Pearson correlation coefficient of 0.9924 in DCNN regression model, there is a strong positive linear relationship between the true definition rate and the predicted definition rate.

Therefore, through DCNN regression model, the spectrogram quality from human activity in terms of definition rate can be evaluated. Indeed, through the implementation of the DCNN regression model, it has been confirmed that the assumption of the definition rate and being equal to the sampling rate is valid. The evaluated spectrogram quality provides clue for how to update the radar parameters to enhance the quality of it for better classification.

In summary, the DCNN regression model allows for the evaluation of spectrogram quality in terms of definition rate, providing valuable insights into the clarity and resolution of the spectrograms. This information can be used to update radar parameters and enhance the quality of the spectrograms, leading to improved classification performance in micro-Doppler analysis of human activity.

Authorized licensed use limited to: Carnegie Mellon University Libraries. Downloaded on November 14,2025 at 13:28:53 UTC from IEEE Xplore. Restrictions apply.

TABLE I
RADAR PARAMETER (f_c) WHEN HUMAN MOTION SPECTROGRAM FOLDING RATE IS 90 AND f_s IS 1 kHz

Human motion	Carrier frequency(GHz)
Run	4.2
Run with box	3.6
Run to crouch	6
Crouch to run	4.8
Skipping	11
Walk	13.5
Walk2hop2walk	6

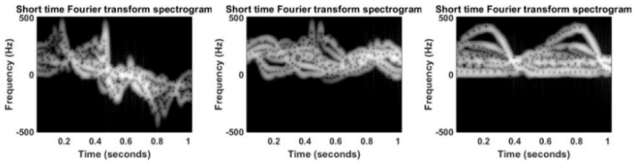

Fig. 8. Human motion spectrogram whose folding rate is 90. (a) Run. (b) Skipping. (c) Walk.

V. IMAGE QUALITY AND DCNN PERFORMANCE

Before applying RL to optimize the radar parameters, it is necessary to find the relation between image quality, i.e., folding rate and definition rate, and DCNN classification accuracy. Even though we have assumed the correlation between them, it has not been verified yet. Through this test, we can ensure that the image quality significantly affects the classification rate.

We compare its classification accuracy depending on the folding rate through Alexnet. As each motion has different velocities, each motion has different f_C values that lead to identical folding rate. For example, Fig. 8 shows human motion spectrogram when folding rate is set to 90. Table I shows its corresponding required f_C for each activity when f_S is 1 kHz.

The images with identical folding rate were classified using Alexnet, setting input size [227 227 3]. By generating 50 spectrograms for each seven distinct motions, the ratio between train data and validation data was 0.76:0.24. Fig. 9 shows the classification accuracy when folding rate is identical among seven different motions. This result indicates that there is a specific range of folding rate that increases the classification performance. As the folding rate closes to 100, the accuracy was maximized. Therefore, we use the folding rate of 90 to have a margin as the folding rate from DCNN has an error.

The fact that data consist of folding rate above 90 increases the overall classification accuracy can also be verified by analyzing individual motion classification performance. While Fig. 5 shows the average classification performance among seven distinct human motions in Section III, we separate Fig. 5 into individual motion classification performance to figure out the individual motion classification performance depending on radar parameters. Fig. 10 shows run, crouchtorun, and walk2hop2walk motion classification performance.

From Fig. 10 and Table I, higher classification performance is observed in the range, where the carrier frequency results in above 90. As the velocity of human limb motion is faster

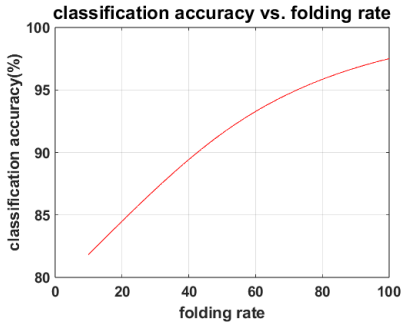

Fig. 9. Classification accuracy with different folding rates when sampling rate is 1 kHz.

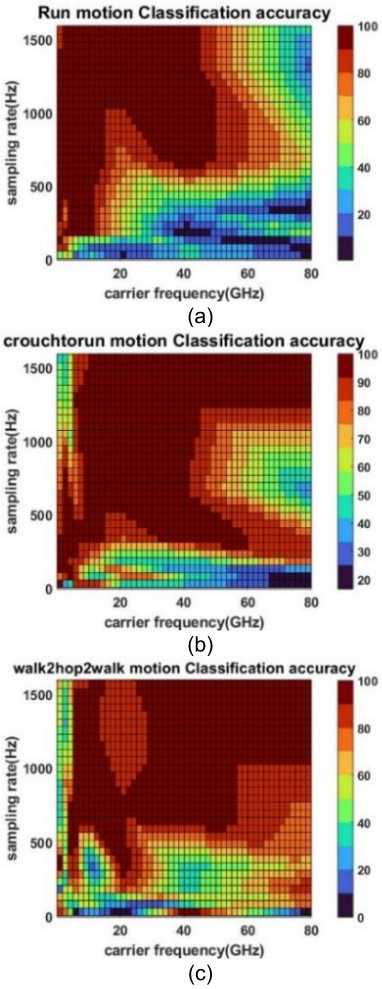

Fig. 10. Individual motion classification accuracy as radar parameters change. (a) Run (b) Crouch to run. (c) Walk2hop2walk.

for the running activity, crouch to run and walk2hop2walk, the result indicates that low-speed human motions require higher carrier frequencies to achieve a folding rate above 90. Therefore, in order to achieve higher classification performance in detecting individual motions, it is necessary to ensure a folding rate above 90.

An analogous trend can be found for the definition rate, i.e., sampling rate. From Fig. 10, it is observed that it is necessary to have a sampling rate that is above a certain level depending on the kinds of activity as well as the carrier

Authorized licensed use limited to: Carnegie Mellon University Libraries. Downloaded on November 14,2025 at 13:28:53 UTC from IEEE Xplore. Restrictions apply.

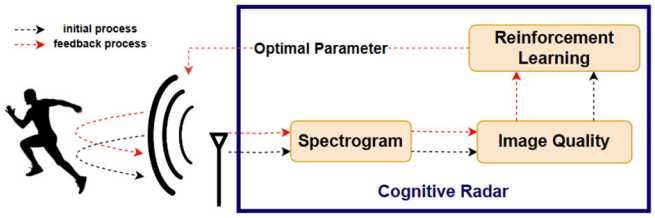

Fig. 11. Working procedure of trained cognitive radar.

frequency. This implies the existence of an optimal definition rate that yields high classification accuracy. Furthermore, the classification accuracy is not solely influenced by the definition rate but also by the interplay between the sampling rate and carrier frequency. The combination of these two parameters plays a significant role in determining the individual motion classification performance.

The overall result in this section suggests that the high image quality is closely associated with better classification accuracy. Specifically, the results indicate that the classification performance tends to be higher when the folding rate falls within the range of 90–100. This indicates that a well-defined and nonaliased spectrogram, characterized by a folding rate above 90, is crucial for accurate micro-Doppler classification. Therefore, adjusting radar parameters to enhance spectrogram quality is a crucial direction for improving classification performance. By optimizing the radar parameters to achieve higher image quality, we can effectively enhance the accuracy of micro-Doppler classification. Given the intricate relationship between radar parameters and image quality, the utilization of RL for optimizing these parameters becomes necessary.

VI. RL for Cognitive Radar

A. Concepts of Cognitive Radar

We employ the cognitive radar scheme to maximize the accuracy of human motion classification. Cognitive radar is an advanced radar system that incorporates adaptive learning and intelligent decision-making to enhance radar performance. In this study, cognitive radar scheme evaluates the environment, i.e., the spectrogram quality depending on human motion, and adjusts the radar parameters to have a spectrogram with better quality. We introduce RL to implement cognitive radar [18]. When unknown motion is detected, the quality of image is determined through the DCNNs. Then, RL finally determines the better radar parameters based on its evaluated spectrogram quality to enhance it, as shown in Fig. 11.

RL is implemented by formulating the problem as a Markov decision process (MDP). In RL, the states, actions, and rewards are specified. State represents the configuration of the environment. They capture all relevant information needed for decision-making. In this research, a state describes the current setup of our radar system and the data it is processing. Action is a decision made by RL agent based on the current state. In this research, actions correspond to the radar parameter settings, such as f_C and f_S. Reward is scalar feedback made by the RL agent after it takes an action. In this research, rewards are computed based on factors, such as folding rate, definition rate, accuracy, and the step taken in the RL process. Among many RL algorithms, we employed Q-learning, which is used to solve MDP without prior knowledge [19]. It is a value-based method that learns an optimal action-value function, known as the Q-function, denoted as $Q(S, A)$. The Q-function represents the expected cumulative reward for taking action A in a given state S. It maps a state-action pair (S, A) to the expected cumulative reward. The Q-function is initially initialized randomly, and as the RL agent interacts with the environment, it iteratively updates the Q-function's parameters using the Bellman equation [15]. The equation involves key components

$$Q(S_t, A_t) \leftarrow (1-\alpha) \cdot Q(S_t, A_t) + \alpha\left[R_t + \gamma \cdot Q(S_{t+1}, A_{t+1})\right] \tag{4}$$

where R represents the immediate reward received for taking a specific action A in a given state S. γ is the discount factor that balances the importance of immediate against future rewards. It determines how much weight is given to future outcomes when making decisions. α is the learning rate, which determines the impact of new information on updating the Q-function. It controls the rate of learning and the extent to which the Q-values are adjusted. S_{t+1} represents the next state observed after taking action A in current state S, and A_{t+1} represents the action that maximizes the Q-value in the next state.

TABLE II
EIGHT POSSIBLE COMBINATIONS IN RL ALGORITHM

Radar parameter	Increase	Decrease
Carrier frequency(GHz)	0.5 or 2	0.5 or 2
Sampling rate (Hz)	50 or 500	50 or 500

B. RL Training Process

During the training process, the RL agent interacts with the environment, updates the Q-function, and adjusts its behavior to maximize the expected cumulative reward. By repeating this process and refining the Q-function through exploration and exploitation, the RL agent gradually learns the optimal policy for maximizing rewards in the given MDP. In this problem, the state of S is specified by radar parameters of f_C and f_S. The action of A consists of eight possible actions, each corresponding to adjusting f_C and f_S shown in Table II.

Reward function is determined by its image quality, i.e., folding rate and definition rate, and the classification accuracy described in Fig. 5. The explanation is shown in Fig. 12. By setting the environment where maximum f_C is 80 GHz and f_S is 2 kHz, Q-learning is trained.

In the training process, two Q-functions are initialized, one for f_C and f_S and another one for folding rate and definition rate. Then, we set the hyperparameters for the algorithm, such as learning rate (α), discount factor (γ), and exploration rate (ε). Algorithm is initiated for 15 000 episodes. Each episode randomly selects the radar parameters. The algorithm then takes the action using an epsilon-greedy policy to select

Authorized licensed use limited to: Carnegie Mellon University Libraries. Downloaded on November 14,2025 at 13:28:53 UTC from IEEE Xplore. Restrictions apply.

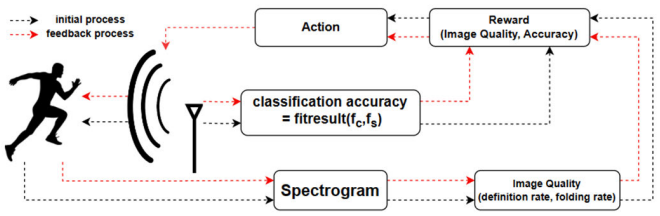

Fig. 12. Structure of RL for training the cognitive radar.

action at each step with a maximum value of 100

$$A \leftarrow \begin{cases} \underset{a}{\text{argmax}}\left\{Q_{\text{freq,samp}}(S, A) + Q_{\text{fold,def}}(S, A)\right\}, & \in \geq \varepsilon \\ \text{random action}, & \in \leq \varepsilon. \end{cases} \tag{5}$$

After action A is selected, the reward is calculated by defined reward function R (folding rate, definition rate, accuracy, and step). Reward is given based on the image quality we have discussed on Section V. The desired range of folding rate is set between 90 and 100. We have defined the most desirable folding rate as 100. If the folding rate deviates from this range, the reward function responds with penalties. These penalties are determined by the absolute difference between the idealized folding rate and observed folding rates, scaled by a factor of 100 and negated. This discourages significant deviations from the desired folding rate. Conversely, a reward is applied and calculated as a function of the desired value divided by the absolute difference between the desired and observed folding rates. This encourages the agent to maintain the folding rate within the target range, with rewards increasing as the rate approaches the desired level.

Considering the definition rate, if the rate increases, image quality increases. However, as the rate increase, it also accompanied with longer computing time occurred by hardware which is a penalty. Therefore, the desired range of definition rate is set between 500 and 1000. We have defined the most desirable definition rate as 500. If the definition rate deviates from this range, the reward function responds with penalties. The penalties are determined by the absolute difference between the target desired definition rate and observed definition rate, normalized by the desired definition rate. This encourages the agent to maintain definition rate within the specific range. When the observed definition rate exceeds the desired definition rate, a reward is issued. The reward is calculated based on the absolute difference between the desired definition rate and observed definition rate, normalized by the desired definition rate. This encourages the agent to maintain definition rate above the desired definition rate.

Lastly, the change in accuracy between consecutive steps to reflect the system's performance is considered. We have defined step size, which represents the number of steps taken during RL training, divided by 100. A reward is given when accuracy improves with the reward magnitude being proportional to the absolute change in accuracy, scaled by a factor of five times the step size. Conversely, penalties are applied when accuracy decreases, with the penalty magnitude being proportional to the absolute change in accuracy, scaled by a factor of five times the step size. This encourages the agent to prioritize actions that enhance the radar system's overall performance and penalizes actions that lead to performance degradation.

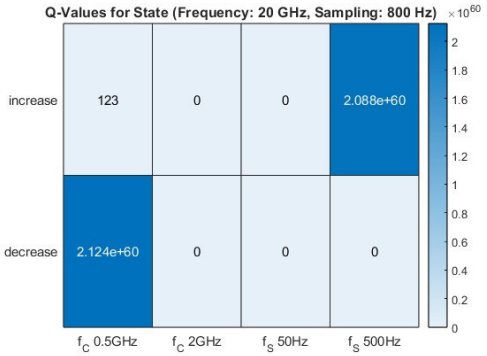

Fig. 13. Q-values for eight possible actions when $f_C = 20$ GHz and $f_S = 800$ Hz.

Based on the state, action, and reward, Q-function is updated according to Bellman equation

$$Q_{\text{freq,samp}}(S_t, A_t) \leftarrow (1-\alpha)\cdot Q_{\text{freq,samp}}(S_t, A_t) + \alpha\left[R_t + \gamma \cdot Q_{\text{freq,samp}}(S_{t+1}, A_{t+1})\right] \tag{6}$$

$$Q_{\text{fold,def}}(S_t, A_t) \leftarrow (1-\alpha)\cdot Q_{\text{fold,def}}(S_t, A_t) + \alpha\left[R_t + \gamma \cdot Q_{\text{fold,def}}(S_{t+1}, A_{t+1})\right]. \tag{7}$$

Fig. 13 represents the Q-values for specific state-action pairs. In the Q-learning algorithm, the action selection is typically based on the maximum Q-value for a particular state. Based on this figure, when f_C is 20 GHz and f_S is 800 Hz, decreasing f_C by 0.5 GHz is the most optimal action to take.

C. RL Verification

After training the Q-function, we verify the performance of the trained RL algorithm. We have set up a situation in which human motion persists long enough to be detected by the radar and for its radar parameters to be optimized for classification.

In our evaluation of the stability of our RL model, we conducted a learning curve analysis. Fig. 14 displays the average value per episode. To gain a more detailed understanding of the observed trend, we employed a curve fitting procedure. Specifically, we used the optimization algorithm known as "NonlinearLeastSquares." This algorithm iteratively refines the parameters of a Gaussian curve to minimize the disparities between the curve and the actual data points. Notably, as the number of episodes increases, the learning curve exhibits a trend toward convergence. This convergence pattern indicates that the RL model has reached a stable state.

Also, we set four environments, which are involved with poor spectrogram qualities and observe how RL determines the radar parameters. Results are shown in Figs. 15–18. The first environment scenario is when $f_C = 1$ GHz and $f_S = 2000$ Hz, which corresponds to the folding rate $= 2$ and definition rate $= 2000$. When testing the environment through RL, after 14 steps, radar has finally reached to its optimal parameters showing 98.3% classification accuracy. The final environment of the agent is when $f_C = 17$ GHz, $f_S = 1450$ Hz, folding

Authorized licensed use limited to: Carnegie Mellon University Libraries. Downloaded on November 14,2025 at 13:28:53 UTC from IEEE Xplore. Restrictions apply.

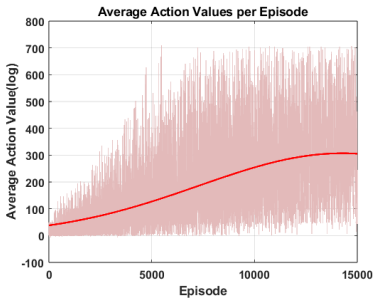

Fig. 14. Learning curve of RL.

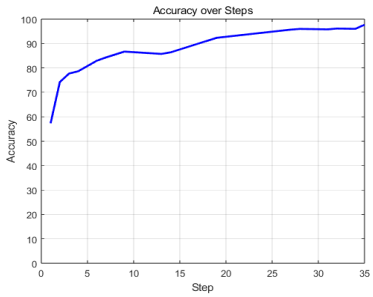

Fig. 15. Environment when $f_C = 1$ GHz, $f_S = 2000$ Hz, folding rate $= 2$, and definition rate $= 2000$.

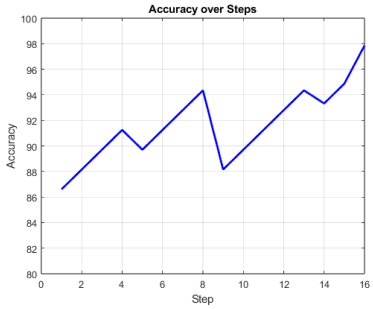

Fig. 16. Environment when $f_C = 5$ GHz, $f_S = 300$ Hz, folding rate $= 200$, and definition rate $= 300$.

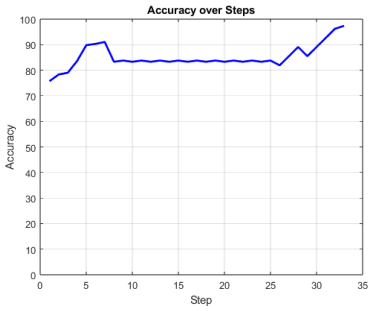

Fig. 17. Environment when $f_C = 0.5$ GHz, $f_S = 320$ Hz, folding rate $= 20$, and definition rate $= 320$.

rate $= 92$, and definition rate $= 1450$. The second environment scenario is when $f_C = 5$ GHz and $f_S = 300$ Hz, which corresponds to folding rate $= 200$ and definition rate $= 300$. When testing the environment through RL, after 16 steps, radar has finally reached its optimal parameters showing 97.85% classification accuracy. The final environment of the agent is when $f_C = 8$ GHz, $f_S = 1250$ Hz, folding rate $= 72$, and

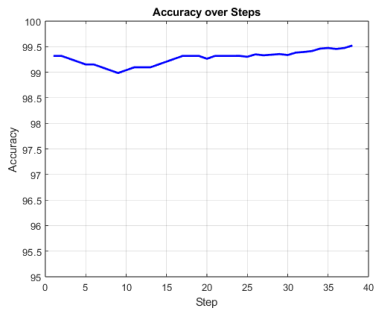

Fig. 18. Environment when $f_C = 74$ GHz, $f_S = 2000$ Hz, folding rate $= 200$, and definition rate $= 2000$.

definition rate $= 1250$. The third environment scenario is when $f_C = 0.5$ GHz and $f_S = 320$ Hz, which corresponds to folding rate $= 20$ and definition rate $= 320$. When testing the environment through RL, after 34 steps, radar has finally reached its optimal parameters showing 97.4% classification accuracy. The final environment of the agent is when $f_C = 7$ GHz, $f_S = 1270$ Hz, folding rate $= 61$, and definition rate $= 1270$. The last environment scenario is when $f_C = 74$ GHz and $f_S = 2000$ Hz, which corresponds to folding rate $= 2$ and definition rate $= 2000$. When testing the environment through RL, after 38 steps, radar has finally reached its optimal parameters showing 99.5% classification accuracy. The final environment of the agent is when $f_C = 24.5$ GHz, $f_S = 1850$ Hz, folding rate $= 113$, and definition rate $= 1850$.

Based on the radar optimization in four distinct environments shown above, the spectrogram changes according to its final environment of the agent. Table III illustrates the changes in the micro-Doppler signature before and after the application of RL for the four environments mentioned above.

Table III indicates that radar parameter is optimized based on its image quality, which results in DCNN performance. In case 1, when folding rate is extremely low and definition rate is extremely high, RL tends to optimize the radar parameters by increasing its folding rate and decreasing its definition rate. In case 2, when folding rate is extremely high and definition rate is extremely low, RL tends to optimize the radar parameters by decreasing its folding rate and increasing its definition rate. In case 3, when folding rate is extremely low and definition rate is extremely low, RL tends to optimize the radar parameters by increasing its folding rate and increasing its definition rate. In case 4, when folding rate is extremely high and definition rate is extremely high, RL tends to optimize the radar parameters by decreasing its folding rate and decreasing its definition rate.

These tests demonstrate the capability of RL to effectively determine the optimal radar parameters that maximize the performance of the DCNN model for human classification. RL's adaptability and ability to evaluate spectrogram quality through the DCNN regression models empower it to make informed decisions and fine-tune the radar parameters to suit the specific requirements of each scenario.

However, it is important to note that there may be fluctuations in accuracy with each step, despite the overall increasing trend. This variation can be attributed to the inherent error present in Fig. 7. These errors introduce uncertainties in the estimation of definition rate, which in turn may affect the

Authorized licensed use limited to: Carnegie Mellon University Libraries. Downloaded on November 14,2025 at 13:28:53 UTC from IEEE Xplore. Restrictions apply.

TABLE III
IMAGE BEFORE OPTIMIZATION AND IMAGE AFTER OPTIMIZATION

	Image before optimization	Image after optimization
Case 1	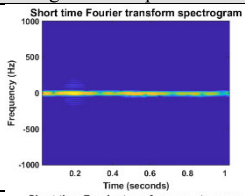	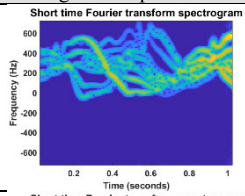
Case 2	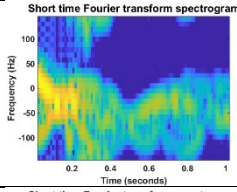	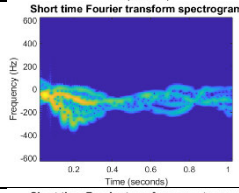
Case3	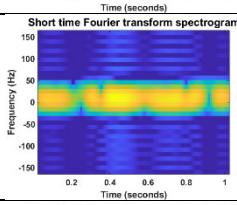	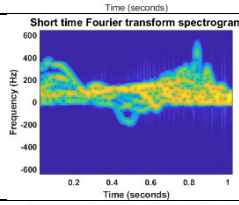
Case4	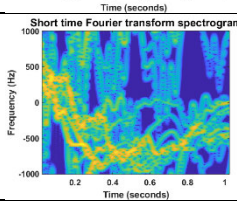	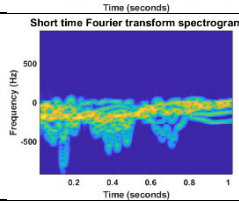

accuracy to some extent. Nonetheless, the consistent upward trend in accuracy reaffirms the efficacy of RL in optimizing radar parameter for improved micro-Doppler classification performance.

VII. CONCLUSION

In this article, we investigated the implementation of cognitive radar to increase the accuracy of human motion classification by optimizing carrier frequency and sampling rate. Analyzing the relationship between classification performance and radar parameters was observed that specific combination of f_C and f_S led to improved classification accuracy. To further improve the radar performance, RL was employed to adaptively adjust the radar parameters based on the evaluated spectrogram quality.

Through the RL algorithm, the cognitive radar system effectively learned and optimized the radar parameters, resulting in enhanced classification accuracy of micro-Doppler signatures. The RL agent successfully adjusts f_C and f_S in a way that maximizes the image quality, as indicated by the folding rate and definition rate, leading to improved classification performance. The trained RL algorithm demonstrates its ability to dynamically adapt the radar parameters based on the environment and the quality of the spectrogram.

The findings of this research contribute to the advancement of cognitive radar systems for micro-Doppler classification. By incorporating RL, the cognitive radar scheme showed its potential in optimizing radar parameters to achieve high accuracy in classifying different human motions. This result emphasizes the importance of considering spectrogram quality and its impact on classification accuracy, and the effectiveness of RL in determining optimal radar parameters based on the evaluated image quality. It also highlights the concept's feasibility through RL simulation based on measured data.

However, there are some limitations to our study. In a real-time situation, rapid changes in human motion pose a challenge due to a delay in the optimization process through RL. RL requires several observations to find optimal parameters. Additionally, hardware constraints may cause delays in creating human motion spectrograms from received signals. Thus, scenarios where human motion persists for extended periods are more suitable in this context.

Further research is necessary to address these limitations, such as minimizing computational time to enhance classification performance immediately. Additionally, we have focused on only two parameters, the definition rate and folding rate, as indicators of image quality. Yet, expanding the scope to include parameters, such as STFT dwell time, overlap rate in STFT, and polarization, which affect the spectrogram, may provide valuable insights for optimizing parameters to enhance classification performance.

Moreover, considering that we have employed an RL algorithm, which is a value-based method, we suggest that a policy gradient model could be effectively applied to this situation. Given that the optimization of parameters is in a continuous context, policy-based methods have the potential to minimize step size and, in turn, optimize radar parameters more efficiently.

In conclusion, this study highlights the potential of cognitive radar with RL for improving the accuracy of micro-Doppler classification, providing valuable insights into the design and optimization of radar systems for effective human motion analysis and recognition. It also underscores the need for addressing real-time challenges and broadening the scope of parameters for further research. Further investigation is warranted to ascertain the software's compatibility and functionality within the broader context of software-defined radio (SDR). This research offers a strong foundation for future work in the field of cognitive radar, which can explore more complex motion patterns, different RL algorithms, and applications beyond human motion classification, ultimately enhancing radar performance across various domains.

REFERENCES

[1] B. Jokanovic, M. Amin, and B. Erol, "Multiple joint-variable domains recognition of human motion," in *Proc. IEEE Radar Conf. (RadarConf)*, Seattle, WA, USA, May 2017, pp. 0948–0952.

[2] M. Muqtadir, M. H. Butt, D. Qazi, F. A. Butt, I. H. Naqvi, and N. U. Hassan, "Health secure radar: Use of micro Doppler signatures for health care and security applications," in *Proc. IEEE VTS 17th Asia–Pacific Wireless Commun. Symp. (APWCS)*, Osaka, Japan, Aug. 2021, pp. 1–6.

[3] S. Björklund, H. Petersson, A. Nezirovic, M. B. Guldogan, and F. Gustafsson, "Millimeter-wave radar micro-Doppler signatures of human motion," in *Proc. 12th Int. Radar Symp. (IRS)*, Leipzig, Germany, Sep. 2011, pp. 167–174.

[4] D. P. Fairchild and R. M. Narayanan, "Classification of human motions using empirical mode decomposition of human micro-Doppler signatures," *IET Radar, Sonar Navigat.*, vol. 8, no. 5, pp. 425–434, Jun. 2014.

[5] Y. Kim and T. Moon, "Human detection and activity classification based on micro-Doppler using deep convolutional neural networks," *IEEE Geosci. Remote Sens. Lett.*, vol. 13, no. 1, pp. 8–12, Jan. 2016.

Authorized licensed use limited to: Carnegie Mellon University Libraries. Downloaded on November 14,2025 at 13:28:53 UTC from IEEE Xplore. Restrictions apply.

[6] G. Klarenbeek, R. I. A. Harmanny, and L. Cifola, "Multi-target human gait classification using LSTM recurrent neural networks applied to micro-Doppler," in *Proc. Eur. Radar Conf. (EURAD)*, Oct. 2017, pp. 167–170.

[7] B. Erol, S. Z. Gurbuz, and M. G. Amin, "Motion classification using kinematically sifted ACGAN-synthesized radar micro-Doppler signatures," *IEEE Trans. Aerosp. Electron. Syst.*, vol. 56, no. 4, pp. 3197–3213, Aug. 2020.

[8] R. J. Abad, M. H. Ierkic, and E. I. Ortiz-Rivera, "Basic understanding of cognitive radar," in *Proc. IEEE ANDESCON*, Oct. 2016, pp. 1–4.

[9] S. Z. Gurbuz, H. D. Griffiths, A. Charlish, M. Rangaswamy, M. S. Greco, and K. Bell, "An overview of cognitive radar: Past, present, and future," *IEEE Aerosp. Electron. Syst. Mag.*, vol. 34, no. 12, pp. 6–18, Dec. 2019.

[10] Y. Kim and H. Ling, "Human activity classification based on micro-Doppler signatures using a support vector machine," *IEEE Trans. Geosci. Remote Sens.*, vol. 47, no. 5, pp. 1328–1337, May 2009.

[11] J. R. Guerci, R. M. Guerci, M. Ranagaswamy, J. S. Bergin, and M. C. Wicks, "CoFAR: Cognitive fully adaptive radar," in *Proc. IEEE Radar Conf.*, Cincinnati, OH, USA, May 2014, pp. 0984–0989.

[12] C. E. Thornton, M. A. Kozy, R. M. Buehrer, A. F. Martone, and K. D. Sherbondy, "Deep reinforcement learning control for radar detection and tracking in congested spectral environments," *IEEE Trans. Cognit. Commun. Netw.*, vol. 6, no. 4, pp. 1335–1349, Dec. 2020.

[13] L. O. Wabeke and W. A. J. Nel, "Utilizing Q-learning to allow a radar to choose its transmit frequency, adapting to its environment," in *Proc. 2nd Int. Workshop Cognit. Inf. Process.*, Elba, Italy, Jun. 2010, pp. 263–268.

[14] M. Kozy, J. Yu, R. M. Buehrer, A. Martone, and K. Sherbondy, "Applying deep-Q networks to target tracking to improve cognitive radar," in *Proc. IEEE Radar Conf. (RadarConf)*, Boston, MA, USA, Apr. 2019, pp. 1–6.

[15] S. S. Ram, C. Christianson, Y. Kim, and H. Ling, "Simulation and analysis of human micro-Dopplers in through-wall environments," *IEEE Trans. Geosci. Remote Sens.*, vol. 48, no. 4, pp. 2015–2023, Apr. 2010.

[16] S. S. Ram and H. Ling, "Simulation of human microDopplers using computer animation data," in *Proc. IEEE Radar Conf.*, Rome, Italy, May 2008, pp. 1–6.

[17] J. Li, X. Chen, G. Yu, X. Wu, and J. Guan, "High-precision human activity classification via radar micro-Doppler signatures based on deep neural network," in *Proc. IET Int. Radar Conf. (IET IRC)*, vol. 2020, Nov. 2020, pp. 1124–1129.

[18] X. Shichao, Z. Qun, L. Ying, and L. Kaiming, "Reinforcement learning based waveform design for cognitive imaging radar," in *Proc. IEEE 3rd Int. Conf. Electron. Inf. Commun. Technol. (ICEICT)*, Shenzhen, China, Nov. 2020, pp. 568–573.

[19] Z. Qu, C. Hou, C. Hou, and W. Wang, "Radar signal intra-pulse modulation recognition based on convolutional neural network and deep Q-learning network," *IEEE Access*, vol. 8, pp. 49125–49136, 2020.

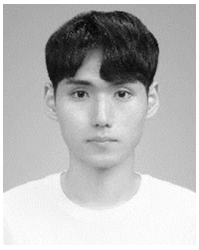

Amin Hong (Student Member, IEEE) is currently pursuing the B.S. degree with the Department of Electronic Engineering, Sogang University, Seoul, South Korea.

His primary topic of research lies in the application of cognitive radar for micro-Doppler classification. Other topics of interests include radar image processing and deep learning application for target detection.

Young-Hoon Chun (Member, IEEE) received the M.S. and Ph.D. degrees in electronic engineering from Sogang University, Seoul, South Korea, in 1995 and 2000, respectively.

From 2000 to 2005, he was a Research Staff with the Millimeter-Wave Innovation Technology (MINT) Research Center, Dongguk University, Seoul. During 2004, he was a Visiting Scholar with Heriot-Watt University, Edinburgh, U.K. He worked with the Department of Electronic Engineering, Heriot Watt University, as a Research Associate, from 2005 to 2008. Since 2009, he has been with LIG Nex1, Yongin, South Korea, as a Principal Research Engineer. His research interests include advanced radar system and subsystems.

Sangyeol Oh received the Ph.D. degree in computer and radio communications engineering from Korea University, Seoul, South Korea, in 2019.

In 2019, he joined the Korea Electrotechnology Research Institute (KERI), Changwon, South Korea, as a Postdoctoral Research Associate, where he was involved in the design of microwave power transmission systems. In 2022, he joined the LIG Nex1, Yongin, South Korea, as a Senior Research Engineer. His current research interests include microwave photonics radar and cognitive radar.

Youngwook Kim (Senior Member, IEEE) received the B.S. degree in electrical engineering from Seoul National University Seoul, South Korea, in 2003, and the M.S. and Ph.D. degrees in electrical and computer engineering from the University of Texas at Austin, Austin, TX, USA, in 2005 and 2008, respectively.

He worked at the Department of Electrical and Computer Engineering, California State University, Fresno, CA, USA, from 2008 to 2021. From 2022, he works as a Professor with Sogang University, Seoul. He has published more than 100 technical papers. His research interests include the area of radar signal processing, antenna design, and RF electronics. His primary topic of research lies in radar target classification with machine-learning techniques. Currently, remote detection, monitoring, and analysis of human motions using EM wave have been focused in his research with deep learning algorithms.

Dr. Kim was a recipient of the Provost Award for Research, Scholarship and Creative Accomplishment, the LCOE Outstanding Research Award, the Claude Laval Jr. Award, Provost's New Faculty Award from the California State University, the A.D. Hutchison Fellowship from the University of Texas at Austin, and the National IT Fellowship from the Ministry of Information and Communication, South Korea.

Authorized licensed use limited to: Carnegie Mellon University Libraries. Downloaded on November 14,2025 at 13:28:53 UTC from IEEE Xplore. Restrictions apply.